Icelandic Low Cyclone Activity: Climatological Features, Linkages with the NAO, and Relationships with Recent Changes in the Northern Hemisphere Circulation

MARK C. SERREZE, FIONA CARSE, AND ROGER G. BARRY

Cooperative Institute for Research in Environmental Sciences, Division of Cryospheric and Polar Processes, University of Colorado, Boulder, Boulder, Colorado

JEFFREY C. ROGERS

Department of Geography, Ohio State University, Columbus, Ohio

(Manuscript received 16 November 1995, in final form 24 June 1996)

ABSTRACT

Output from a cyclone detection and tracking algorithm, applied to twice-daily sea level pressure (SLP) fields for the period 1966–93, is used to examine the characteristics of cyclone activity associated with the locus of the mean Icelandic low (IL), variability during extremes of the North Atlantic oscillation (NAO), and recent changes in relation to circulation over the Northern Hemisphere.

Cyclone events within the climatological IL display a modest seasonal cycle with a winter maximum. However, winter systems are considerably deeper than their summer counterparts with much larger maximum deepening rates. During the cold season (October–March), IL cyclone intensities are typical of oceanic systems but exhibit lower maximum deepening rates. During the warm season (April–September), intensities are typical of Northern Hemisphere values with deepening characteristics similar to those for all extratropical oceans. Depending on the month, 10%–15% (13%–18%) of cyclone events in the IL region represent local cyclogenesis (cyclolysis). Roughly half of all IL cyclones correspond to systems showing their first appearance of a closed isobar north of 55°N, but some can be traced upstream as far as the southern and northern Rocky Mountains.

There is a twofold decrease in cold season cyclone events within the climatological IL during negative extremes of the NAO, with accompanying reductions in intensity, but little change in maximum deepening rates or source regions. This is associated with modest increases in activity to the south over a large area from Labrador eastward to Portugal, reflected in the southward excursion and weakening of the subpolar low. Despite a change toward a more positive NAO index in recent years, no significant increases in cold season cyclone activity are observed in the IL region. However, there have been significant local increases within the region north of 60°N for both cold and warm seasons. These are most pronounced over the central Arctic Ocean, associated with decreases in high-latitude SLP of up to 4 mb. The regional patterns of altered cyclone activity and SLP are consistent with recent changes in high-latitude sea ice conditions and surface temperatures.

1. Introduction

The Icelandic low (IL) represents one of the six ''centers of action'' in the Northern Hemisphere circulation, along with the Azores, Pacific, and winter Siberian highs and the Aleutian and summer Asian lows. The IL has long been regarded as a semipermanent low pressure cell in the North Atlantic, typically located between Iceland and southern Greenland between 60° and 65°N (Sahsamanoglou 1990). In winter, the IL is part of a broad area of low sea level pressure (SLP) dominating subpolar latitudes, maintained in part by low-level thermal effects of the comparatively warm underlying ocean. One of the key features of both the IL and Aleutian lows that supports this idea is the observation that the mean isobars around these lows are parallel to and tightly crowded along the coastlines (Wallace 1983). The IL and Aleutian lows are also located downstream of the major midtropospheric stationary wave troughs, where eddy activity is favored (e.g., Blackmon et al. 1984a). A trough of low pressure typically extends northeastward from Iceland over the Norwegian and Barents Seas. On occasion, a trough extends northward along the west coast of Greenland and Davis Strait. The IL is notably weaker in summer, often appearing as a trough of low pressure centered either west or east of southern Greenland.

Walker (1923) first noted a tendency toward simultaneous strengthening or weakening of the IL and the Azores high (AH), which he named the North Atlantic oscillation (NAO). The positive (negative) mode of the NAO occurs when the IL and AH are simultaneously strong (weak). This teleconnection pattern is generally

Corresponding author address: Dr. Mark C. Serreze, CIRES, Division of Cryospheric and Polar Processes, University of Colorado, Boulder, P.O. Box 449, Boulder, CO 80309-0449.

defined as the normalized SLP difference between Ponta Delgada (Azores) and Akureyri, Iceland, and appears in the first eigenvector in the Northern Hemisphere SLP field for all seasons of the year (Barnston and Livezey 1987; Rogers 1990), accounting for roughly one-third of the variability in the sea level pressure field over the North Atlantic Ocean (Deser and Blackmon 1993). The NAO is most pronounced during the Northern Hemisphere winter (Barnston and Livezey 1987). The IL and AH also tend to be located farther north (south) during the positive (negative) NAO mode (Angell and Korshover 1974). In extreme negative modes, the Atlantic pressure gradient may reverse with high pressure near Iceland and low pressure replacing the AH (Moses et al. 1987).

The NAO has been associated with numerous climatic signals. During the positive mode, temperatures in the Iceland–Greenland region tend to be below average (''Greenland Below''), but above average during the negative mode (''Greenland Above''), with opposing anomalies over northern Europe (Walker and Bliss 1932; van Loon and Rogers 1978). Rogers and van Loon (1979) find that ice extent in Davis Strait is above normal when the IL is anomalously strong with concurrent below-normal ice in the Baltic Sea. Precipitation increases over northwest Africa and the Mediterranean Sea during Greenland Above but decreases around Iceland. Since about 1970, the NAO index during winter has changed to a predominantly positive mode, with some particularly large values since 1980 (Hurrell 1995b). Hurrell argues that recent dry conditions during winter over southern Europe and the Mediterranean; wet conditions from Iceland eastward through Scandinavia; cooling near Greenland and the Mediterranean; and warming over Scandinavia, northern Europe, the Former Soviet Union, and much of central Asia reflect this change.

These studies notwithstanding, comparatively little attention has been paid to understanding the IL in terms of cyclone activity, in particular, the characteristics and source regions of the individual storm systems that contribute to this climatological feature, the linkage between the NAO and cyclone activity, and the extent to which changes in storm activity within the IL region relate to changes elsewhere in the Northern Hemisphere. Northern high-latitude SLP fields depicted by atmospheric general circulation models differ widely in their depiction of the IL (Walsh and Crane 1992). Analysis of the source regions, tracks, deepening, and decay characteristics of IL systems can help to validate current models and identify areas where improvements are needed.

A number of studies (e.g., Whittaker and Horn 1984; Serreze 1995) have examined the IL in terms of cyclone frequencies, cyclogenesis, cyclolysis, and deepening rates but only as part of Northern Hemisphere and Arctic analyses, respectively. Carleton (1988) shows that cyclone activity over the North Atlantic is greater during the positive NAO mode and shifts poleward. Although this study was limited to only two winters of cloud vortex signatures in satellite imagery, Hurrell's (1995a) analysis of the transient eddy forcing of the vorticity balance at 300 mb, based on bandpassed data for 1980–91, confirms this general pattern. Rogers (1990) used data from the *Mariners Weather Log* to examine the distribution of cyclones during extremes of the NAO for January. During the positive phase, the main North Atlantic cyclone track exhibits a pronounced northeastward orientation, parallel to the North American east coast with a cyclone maximum just south of the climatological IL. During the negative phase, an east–west orientation is indicated centered roughly along 45°N latitude.

A 28-yr record (1966–93) of twice-daily cyclone statistics for the Northern Hemisphere has been derived from the application of an automated detection and tracking algorithm to National Meteorological Center (NMC) SLP fields for the 47×51 octagonal grid. We use these data to 1) identify the characteristics of cyclone activity associated with the climatological mean IL, 2) clarify the linkage between extremes of the NAO and North Atlantic cyclone activity, and 3) examine recent changes in IL cyclone activity with respect to the larger Northern Hemisphere circulation. We emphasize the cold season (October–March) for which climate signals associated with variability in the IL tend to be best expressed.

2. The cyclone dataset

The detection and tracking algorithm is largely identical to that of Serreze (1995). Cyclones are identified using a series of search patterns, testing whether a gridpoint SLP value is surrounded by gridpoint values at least 2 mb higher than the central point being tested. Starting on the first 12-h chart (chart 1), each cyclone is ascribed a number. A 3×3 NMC grid array is then centered over each system on the next 12-h chart (chart 2). If a cyclone on chart 1 falls within a given 3×3 array, the chart 2 cyclone at the center of the array is taken to be a continuation of the chart 1 system. This immediately tracks stationary or slow-moving cyclones. It is possible that two or more chart 1 systems could fall within the same 3×3 array, but this was rarely observed. The minimum distances from all remaining untracked systems on chart 2 are then determined with respect to the remaining numbered systems on chart 1. Typically, two or more untracked chart 2 systems have their minimum distance with respect to the same chart 1 system. The number of the chart 1 system is carried over to the closest chart 2 system, provided that the minimum distance between them is less than a specified limit and several other checks involving the 12-h sea level pressure tendency (SLPT) at the cyclone centers for a candidate pairing and the direction of system motion are satisfied. Otherwise, the chart 2 system is taken

as new (cyclogenesis), and successively more distant chart 2 systems are tested in the same manner, up to the distance limit. At the end of the search process, all remaining chart 1 systems that could not be paired with a chart 2 system are considered to have filled (cyclolysis). The process is then repeated for each subsequent pair of charts. If any chart is missing, all systems on the next available chart are taken as new and numbered accordingly.

From a one-month comparison with manual analyses, Serreze (1995) found this ''nearest neighbor'' approach [see for comparison the algorithms of Murray and Simmonds (1991) and Sinclair (1994)] tracked systems correctly better than 98% of the time. This essentially reflects the tendency for the distances that individual cyclones move in 12 h to be much smaller than the typical separation between cyclones on a given chart. Nevertheless, the present algorithm includes a number of improvements from Serreze (1995). Most importantly, the original search limit of 1400 km was reduced to 1200 km, increased to 1250 km north of 60°N, in part adjusting for the larger NMC grid spacing at higher latitudes (grid spacings range from 274 km at 20°N to 408 km at the North Pole). Additional improvements, developed from numerous comparisons with manual analyses, include tests for multiple systems within the original 3×3 search shell and checks on the direction of cyclone migration, in which larger distances are allowed for northward versus southward motion, with accompanying thresholds for westward migration. These changes improve the performance in synoptically ''complex'' situations, such as when two separate systems enclosed by a common isobar merge together or when a ''parent low'' is dissipating in conjunction with separate, but related, development of a new system.

Algorithm outputs include the position and central pressure of each cyclone, whether the observation represents a cyclogenesis or cyclolysis event and the local Laplacian ($\nabla^2 P$, in 10^5 mb m^{-2}) and SLPT [mb (12 h)$^{-1}$] at each cyclone center. The local Laplacian is proportional to the geostrophic relative vorticity and, unlike cyclone central pressure, provides an index of cyclone intensity largely independent of changes in the background pressure field (Murray and Simmonds 1991). In turn, SLPT provides a useful index of synoptic development (Sanders and Gyakum 1980), provided that the decrease in cyclone central pressure is not embedded within a region of generally falling or rising pressure and the storm maintains an approximately constant size through the 12-h analysis period (Roebber 1989). Following Roebber (1984), we adjust all SLPT values by latitude using the relationship $\text{SLPT}_{\text{adj}} = \text{SLPT} \sin \phi_{\text{ref}} / \sin \phi$, where ϕ_{ref} is a reference latitude of 60°N and ϕ is the latitude of the SLPT observation. This accounts for the latitudinal variation in geostrophic wind for a unit pressure gradient. The choice of the reference latitude is arbitrary; 60°N was chosen here following Sanders and Gyakum (1980) and Serreze (1995). As the area represented by an NMC grid increases with latitude, maps of counts of system centers, cyclogenesis, and cyclolysis have also been adjusted to a 60°N reference latitude. We consider only systems lasting at least 24 hours (two charts) and have adjusted all system counts for missing data (representing only about 2% of all days).

We apply the algorithm to the complete 47×51 array but restrict subsequent analysis to north of 30°N, avoiding any risk of ''edge effect'' problems in determining cyclogenesis and cyclolysis (cf. Serreze 1995). Apart from possible temporal inhomogeneities in the data (Trenberth and Olson 1988), smoothing over the relatively coarse NMC grid results in loss in detail compared with the ''true'' field. Furthermore, cyclone central pressures will tend to be overestimated (too high) with this effect increasing poleward. Because of the tendency for greater overestimation of central pressures as systems deepen, SLPT will also tend to be underestimated, with this effect greater for intense systems with strong pressure gradients near their center. It can be argued that the algorithm will tend to depict cyclogenesis (cyclolysis) as occurring after (before) its true occurrence, hence possibly biasing where these events are depicted because of the 2-mb cyclone detection threshold and the relatively coarse NMC grid. Finally, the algorithm is limited to the detection of synoptic-scale systems—mesoscale ''polar lows'' will generally be missed. Tropical cyclones will be detected and tracked, but we make no attempt to differentiate them from extratropical disturbances.

3. Characteristics of the climatological mean Icelandic low

a. Mean cyclone characteristics

Figure 1 shows the mean (1966–93) cold season (October–March) distributions of SLP and latitude-weighted cyclone totals. The mean center of the IL (Fig. 1a) at about 62°N, 35°W (with a central pressure of approximately 1000 mb) corresponds closely to (but is shifted slightly southeast of) the maximum in cyclone activity in this region peaking at over 500 systems (Fig. 1b). The mean low is elongated to the northeast, consistent with the secondary cyclone maximum in the Norwegian seas (>300 systems). Other well-known cyclone maxima are also apparent, such as in the Gulf of Alaska, the lee of the southern Rocky Mountains, and over the Mediterranean. In terms of central pressure, corresponding results for the warm season (April–September) show the IL to be much shallower (Fig. 2a), associated with a general reduction in cyclone activity in this region (Fig. 2b).

To examine characteristics of cyclones corresponding to the climatological mean IL, we adopt a simple regional definition of its position as a fixed 4×3 NMC grid array, which encompasses the position of lowest

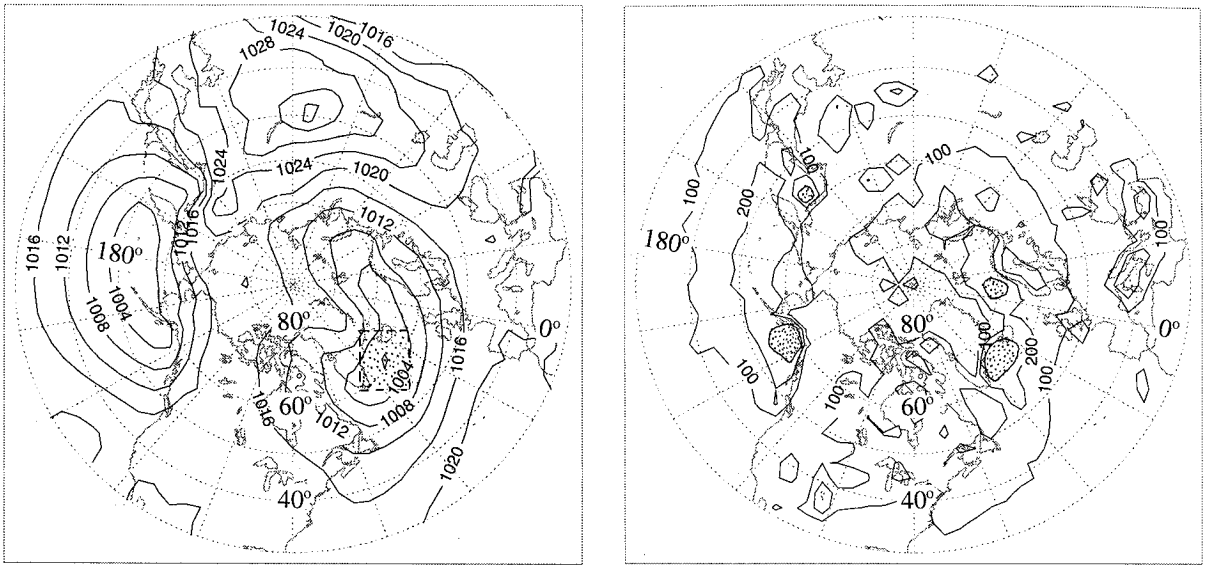

FIG. 1. Distribution of (a) mean SLP and (b) latitude-weighted cyclone events over the period 1966–93 for the cold season. Contour intervals for Fig. 1b are 100, with regions having > 300 systems indicated by stipples. The rectangle in Fig. 1a defines the climatological IL region.

SLP shown in Figs. 1a and 2a. This region, shown in Fig. 1a, includes 60°N, 30°W, the position of highest probability of occurrence of the IL (34.2%) based on minimum pressure positions from annual means and approximately 63% of all annual mean locations for the period 1873–1980 (Sahsamanoglou 1990). It also includes the position of minimum pressure in all long-term monthly SLP means based on the 28-yr record except for July. For this month, a mean low is indicated within our climatological region, but with a slightly deeper separate low found just south of Baffin Island. While arguably one could consider the IL to correspond to this latter position, our regional definition allows for an internally consistent assessment of the seasonal cycle in IL cyclone characteristics.

Table 1 provides long-term monthly values for our climatological region of total cyclone events (N, normalized to an average of 30.4 days per month), average cyclone days [C days, 12-h events divided by the total number of 12-h charts (1702), multiplied by 30.4], mean cyclone intensity ($\nabla^2 P$, in 10^5 mb m^{-2}), the 12-hourly mean maximum deepening at the cyclone centers [mb

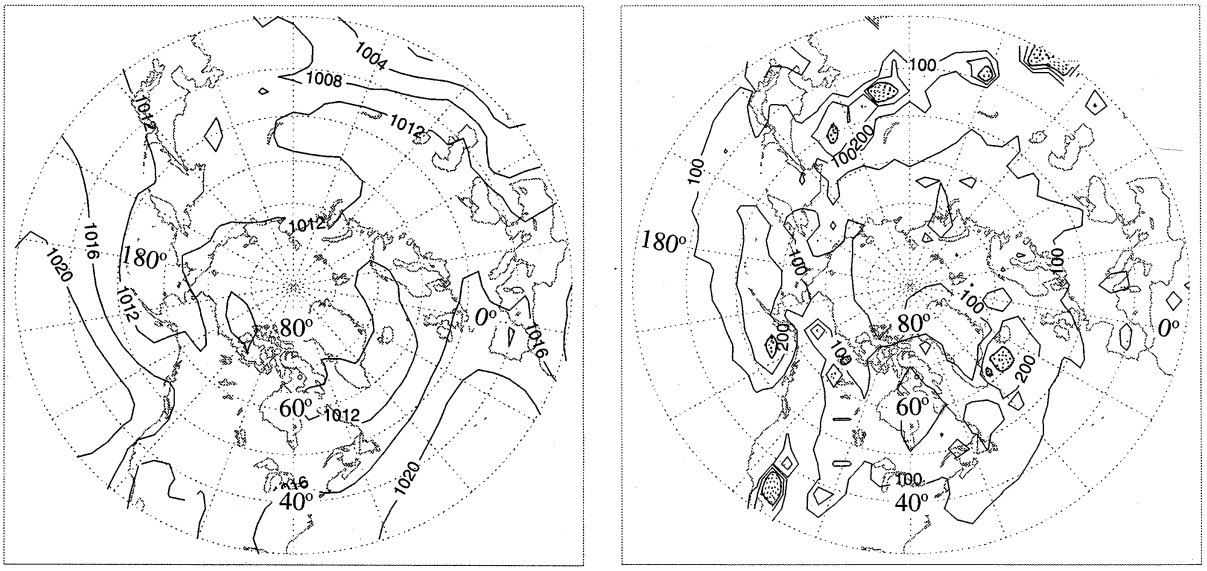

FIG. 2. As in Fig. 1 but for the warm season.

TABLE 1. Seasonal cycle of Icelandic low cyclone characteristics within the 12-point grid.

	N	C days	$\nabla^2 P$ (10^5 mb m^{-2})	Max deepening [mb (12 h)$^{-1}$]	P_{IL} (mb)
Jan	663	11.8	18.8	−7.1	996.0
Feb	653	11.7	18.8	−8.0	997.9
Mar	697	12.4	18.1	−6.7	1000.5
Apr	574	10.3	15.8	−6.4	1009.8
May	485	8.7	14.1	−5.4	1011.9
Jun	574	10.3	12.5	−4.4	1010.2
Jul	531	9.5	11.6	−3.3	1010.0
Aug	611	10.9	13.3	−4.3	1007.6
Sep	614	11.0	15.2	−6.2	1005.5
Oct	659	11.8	16.6	−6.9	1003.0
Nov	621	11.1	16.8	−8.1	1001.3
Dec	627	11.2	18.8	−6.2	998.2
Annual	609	10.9	15.9	−6.1	1004.3

(12 h)$^{-1}$] and the lowest pressure value (P_{IL}) over the 12 gridpoint region, taken from the long-term monthly means. For the maximum deepening statistics (see Serreze 1995), the 12-h latitude-adjusted SLPT was analyzed through the life history of each system from the central pressure (P) values as $P_t - P_{t-1}$, where t is time. The location of each SLPT observation is taken as that at time t. The observation of maximum deepening is extracted, with all maximum deepening events occurring in our IL region, then averaged. As even a synoptically ''active'' region is likely to have a mix of deepening and filling events, analysis of maximum deepening better identifies those months in which synoptic development is pronounced (Roebber 1984, 1989).

Cyclone events show a minimum during May and a March maximum. Although a t test reveals that the differences in the warm and cold season mean counts is statistically significant (0.01 level), it is only for the 4-month period, April–July, that fewer than 600 systems are present. The expected greater intensity of cold season cyclones is clearly evident in the $\nabla^2 P$ values. Minimum intensities are found during July, with maxima from December through February. In turn, P_{IL} ranges from 1011.9 during May to 996.0 mb in January. Maximum deepening rates are also greatest during the winter months, ranging from −8.1 mb (12 h)$^{-1}$ in November to −3.3 mb (12 h)$^{-1}$ for July. The mean December–February and June–August values are somewhat higher than those reported by Serreze (1995) based on a larger domain encompassing our climatological IL region. Although the seasonal cycle in P_{IL} agrees with that shown by Sahsamanoglou (1990) in displaying a January minimum and a May maximum, our values are higher by several mb in all months. This reflects our use of the lowest pressure within the 12-point region from the 28-yr monthly means compared to Sahsamanoglou's (1990) use of the lowest pressure values from monthly means for individual years. As with cyclone counts, t tests of maximum deepening, cyclone intensity, and P_{IL} between the warm and cold season means are statistically significant at the 0.01 level.

To place IL cyclones in the larger context of Northern Hemisphere systems, for both the cold and warm seasons, we examined the mean intensity of cyclones for all grid locations north of 30°N (Fig. 3a). We also examined the number of events at each grid point showing latitude-adjusted deepening of at least 6 and 12 mb (12 h)$^{-1}$ (taken here as ''pronounced'' and ''extreme'' deepening, respectively) and expressed these as a percentage of all

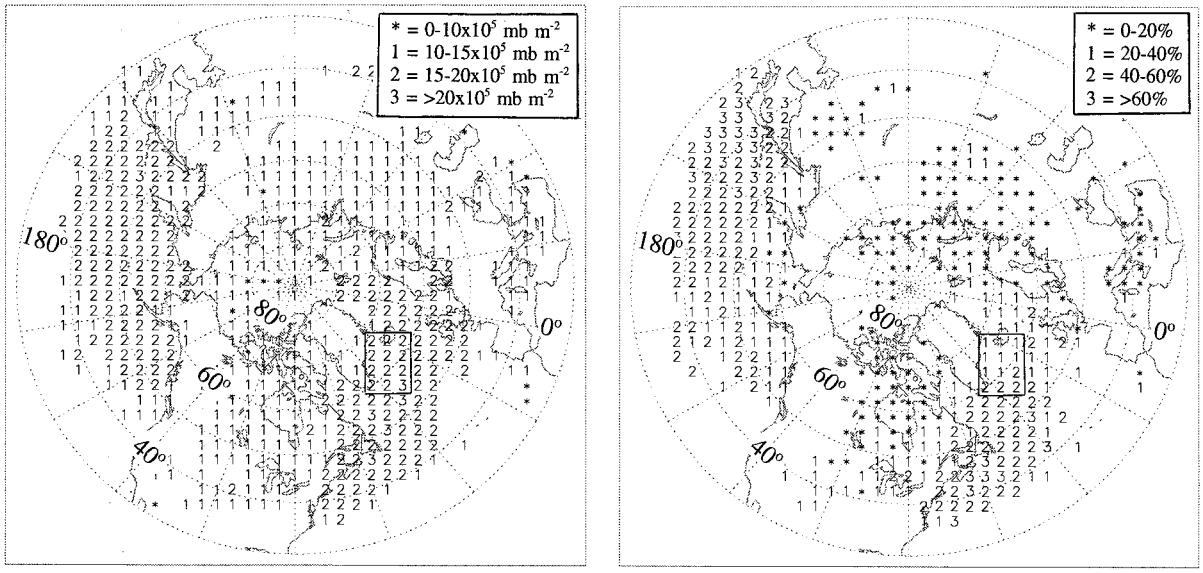

FIG. 3. Cold season distribution of (a) mean cyclone intensity (10^5 mb m^{-2}) and (b) percent occurrence of cyclone deepening >6 mb (12 h)$^{-1}$ with respect to all deepening events. The rectangles define the climatological IL region.

deepening events [SLPT $<$ 0 mb (12 h)$^{-1}$] at that grid point (Fig. 3b). The latter deepening rate, if continued over a day, would correspond to a synoptic ''bomb'' (Sanders and Gyakum 1980) or explosive deepening event. We required that the mean intensity values be based on at least 60 cases and that the deepening percentages be based on at least 30 deepening events.

The difference between oceanic and continental systems for the cold season is shown clearly with respect to both cyclone intensity and pronounced deepening; oceanic systems are generally more intense and show a higher frequency of pronounced deepening (cf. Roebber 1984, 1989). Although the IL region is the locus of peak cyclone activity over the Atlantic (Fig. 1b), the mean intensities of these systems [generally between 15 and 20 ($\times 10^5$ mb m^{-2})] are quite typical of both Atlantic and Pacific storms. With respect to the frequency of pronounced deepening, systems in the southern part of the IL region are fairly typical of most oceanic regions (40%–60%) but are on the lower end (20%–40%) for the northern part and comparable to those associated with the Aleutian low (Figs. 1a and 1b). The highest frequencies of pronounced deepening and extreme deepening events are found east of Honshu, Japan, and along the Atlantic seaboard from about 40°–50°N (see also Roebber 1984). However, extreme deepening events [$>$12 mb (12 h)$^{-1}$] are not uncommon in the IL region with values locally reaching 10%–20%.

Results for the warm season (not shown) indicate the expected sharp reduction in both mean cyclone intensity and the frequency of pronounced deepening events. Icelandic low systems are typical of those over most of the Northern Hemisphere with intensity values between 10 and 15 ($\times 10^5$ mb m^{-2}). There is still a remaining tendency for oceanic systems to exhibit pronounced deepening more frequently, consistent with Roebber's (1989) view that the processes contributing to more rapid development in the marine environment can still be found in summer. However, IL cyclones show a frequency of pronounced deepening on a par with all oceanic regions (up to 40%). Few extreme deepening events occur in the IL region or elsewhere.

b. Cyclone source and decay regions

Earlier studies (Pettersen 1950; Putnins 1970; U.K. Meteorological Office 1974; Whittaker and Horn 1984; Serreze 1995) show the IL to be a synoptically complex region characterized by frequent cyclogenesis, especially during winter. Redevelopment of decaying systems migrating from the south is common and will often be depicted in our database as cyclogenesis events. Cyclogenesis may occur in the cold pool behind occluded cyclones that move northeastward toward Sptizbergen and the Barents Sea. Approaching systems will sometimes show secondary development near the southern tip of Greenland, with one low moving along the west coast into Baffin Bay and the other moving north or northeastward along the east coast and intensifying. Lee cyclogenesis is common under conditions of westerly flow over southern Greenland; redevelopment of lows migrating from the southwest in some cases represents leeside development. In all of these situations, deepening may be rapid as systems draw cold, polar basin air into their circulations. Mesoscale polar lows are also common during winter, but are greatly underrepresented in NMC analyses.

Whittaker and Horn (1984) present maps of mean cyclone tracks and cyclogenesis regions for the four midseason months, based on data from 1958 to 1977. They show that in January, systems found within the IL often originate within the IL itself. They also depict source regions east of Newfoundland and along the seaboard of the eastern United States in January with an additional contribution from the southern Rocky Mountains in April. The contribution from these areas is reduced during July, but with a larger contribution of systems originating east of the northern Rocky Mountains and east of Labrador. Their October results are most similar to those for winter. However, Whittaker and Horn (1984) stress that mean cyclone tracks can be misleading in that relatively few systems ever travel the entire length of the track; most dissipate before the end of the track is reached while others may form along the track and move to the end.

Given the difficulty in interpreting mean storm tracks, it is useful to examine more closely the relative contributions to the IL cyclone maximum represented by local system generation and decay and migration of systems into the IL region from lower latitudes. We tallied separately the number of cyclogenesis and cyclolysis events occurring within our 12-point region, the within-region cyclogenesis events, and all subsequent observations of these systems falling within the 12-point region (Type I events) and those events in the 12-point region for which the cyclogenesis occurred north of 55°N (Type II events). The tallies were then expressed as percentages with respect to all IL cyclone events. We stress that our results apply to lows closed by a 2-mb contour. As noted, many IL cyclogenesis events represent migrating systems that fail to reach the IL as closed lows but that subsequently redevelop in this region. Similarly, some systems displaying cyclolysis within the IL may redevelop in this region and be counted as new cyclogenesis events.

Our results indicate that, depending on the month, 10%–15% of all IL cyclone events represent local cyclogenesis and 13%–18% of events local cyclolysis, with annual averages of 12.4% and 14.3%, respectively. No obvious seasonal cycle is apparent, with *t* tests showing no significant difference between the cold and warm season percentages. Cyclogenesis within the IL and subsequent observations of these systems within the IL (Type I events) account for 14%–22% of all events, with an annual average of 18.4%. However, over 50% of all IL cyclone events correspond to systems showing their

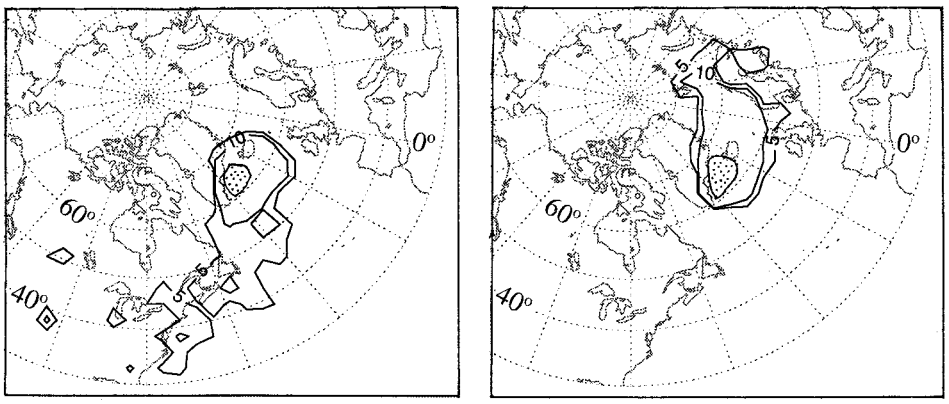

FIG. 4. Cold season distribution of latitude-weighted (a) cyclogenesis and (b) cyclolysis events for systems associated with the IL. Contour intervals are 5 (5–10 events), with regions having >50 events indicated by stipples.

first occurrence of a closed isobar north of 55°N for most months (an annual average of 53.6%), either within or immediately upstream of the IL region. Again, *t* tests show no significant differences in these percentages between the cold and warm seasons.

We next extracted all positions of cyclones that at any point during their lifecycle had at least one observation within the climatological IL region. Figure 4a shows the cyclogenesis locations of these systems for the cold season. In accord with the analyses just described, the primary cyclogenesis region for IL systems is within the IL itself or immediately to the south. Nevertheless, some IL systems can be traced as closed lows to origins as far away as the southern and northern Rocky Mountains, with a larger contribution from the Atlantic seaboard, in broad agreement with the results of Whittaker and Horn (1984). Corresponding results for cyclolysis (Fig. 4b) reveal that systems associated with the mean IL are also most likely to dissipate within the IL region, with the remainder decaying in the Norwegian and Barents Seas. Results for the warm season (not shown) display essentially the same features.

4. Relationships with the NAO

a. Composite analyses

As noted in earlier studies (e.g., Angell and Korshover 1974), the subpolar low tends to both weaken and shift equatorward in the negative mode of the NAO, and vice versa during the positive mode. To address the linkages between these changes and cyclone activity during the cold season, we inspected the monthly NAO index time series from 1966 to 1993 and for each cold season month selected the 7 years with the most positive and most negative index values. The resulting 42 cases for each composite represent the top and bottom quartile values for each month. The composite mean SLP field for the positive NAO extremes (Fig. 5a) shows the central location of the IL lying within the 12-point region

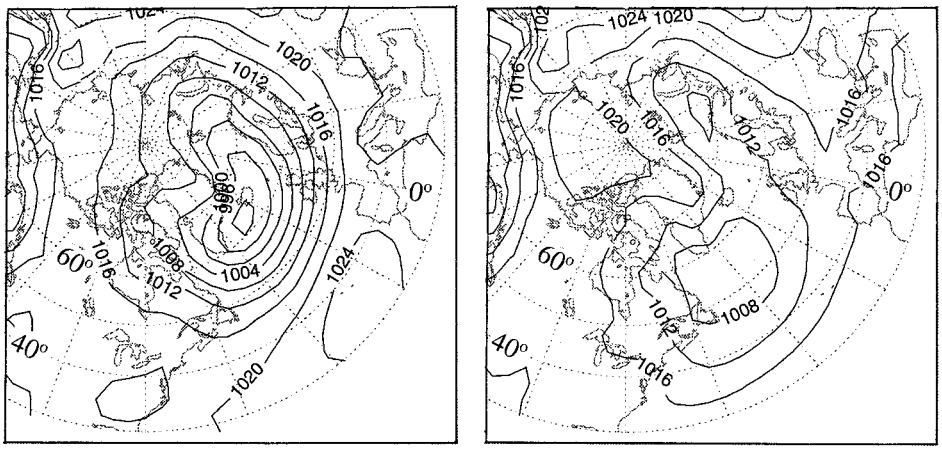

FIG. 5. Cold season mean SLP associated with positive (a) and negative (b) extremes of the NAO index.

TABLE 2. Icelandic low cyclone characteristics under extremes of the NAO Index. Values in parentheses are for the negative mode of the NAO.

	Northern position	Southern position
N	1418 (673)*	535 (644)*
Cyclogenesis (%)	13.0 (14.1)	10.8 (10.9)
Cyclolysis (%)	14.2 (15.1)	13.6 (13.7)
$\nabla^2 P$ (10^5 mb m^{-2})	18.2 (17.0*	19.5 (18.8)
Max deepening [mb (12 h)$^{-1}$]	−8.0 (−6.7)	−10.1 (−8.0)*

* Significant at the 0.01 level.
** Significant at the 0.05 level.

defined in Fig. 1a. Hence, the position of the long-term climatological IL appears to be primarily associated with the positive NAO mode. Figure 5b shows clearly the pronounced southward shift and weakening of the IL during the negative mode of the NAO.

Table 2 summarizes cyclone characteristics corresponding to each composite for the ''northern'' (positive NAO) position of the IL, based on the same 12-point region used in our earlier analyses and the ''southern'' (negative NAO) position, taken as a 4×3 gridpoint region centered over the mean low shown in Fig. 5b. Results for the negative NAO composites are shown in parentheses. No NMC grid points are shared between the two 12-point regions. To assess the statistical significance of the differences between the composite means for each region, monthly time series for each variable and region were first normalized with respect to the long-term (28-yr) monthly means. A two-tailed *t* test was then performed on the departure values corresponding to each composite.

Looking first at the northern position, the obvious change between the positive and negative NAO modes is a statistically significant decrease in cyclone events by more than a factor of 2. Although significant decreases are also observed in the number of cyclogenesis and cyclolysis events (not shown), the percentages of total cyclone events represented by within-region cyclogenesis and cyclolysis are not significantly different. Analysis of the percentages of Type I and Type II cyclone events also reveals no difference (not shown). Cyclones under the positive NAO mode are more intense but exhibit no significant increase in maximum deepening rates. Further analysis of cyclone source and decay regions, identical to those used in Fig. 4, also shows little difference between extremes of the NAO. Consequently, the dominant signal of the NAO in the climatological (also positive NAO) IL region is primarily more systems under the positive mode, which are in turn slightly more intense.

Comparison with the southern position illustrates the southward shift in cyclone activity under the negative NAO mode noted in previous studies (Rogers 1990; Hurrell 1995a). However, the increase in cyclone activity for the negative NAO composite over the southern

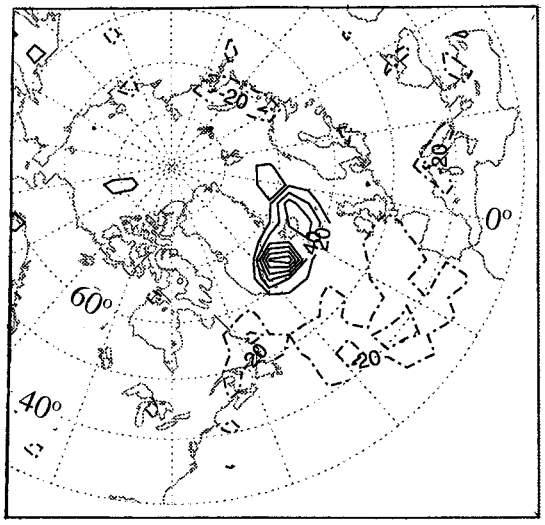

FIG. 6. Positive minus negative NAO difference field of cyclone events for the cold season. The contour interval is 20. Positive differences are shown by solid contours with negative differences shown by dash–dot contours.

region (20%) is quite modest in comparison with the corresponding factor of 2 decrease for the northern region and barely passes significance at the 0.05 level. Note that system counts in the northern region (673) are comparable to those for the southern region (644) during the negative mode. No change in the southern region is noted in other variables, with the exception of significantly smaller maximum deepening rates in the negative mode than in the positive mode.

Figure 6 shows the positive minus negative NAO composite difference field in latitude-weighted cyclone counts. The poleward (equatorward) shift in cyclone activity between the positive (negative) NAO phase is clearly evident and similar to the pattern depicted by Rogers (1990). Under the positive NAO mode, the increase in activity is primarily limited to the climatological IL region itself. Under the negative mode, the increase in activity to the south extends from Labrador eastward to Portugal. Negative differences in cyclone activity under the positive NAO mode are also found over southern Europe and in the Arctic over the Barents and Kara Seas. The changes in cyclone distributions during the negative NAO mode depicted in Table 2 and Fig. 6 are broadly consistent with the southward migration and corresponding weakening of the mean subpolar low (Fig. 5b). However, explanation of the position and strength of the mean low under the negative NAO mode in terms of cyclone counts is clearly incomplete. Note that the largest increases in cyclone counts under the negative NAO mode (Fig. 6) are actually south and east of the center of the mean low (Fig. 5b) and that despite the increases in cyclone activity within the 1008-mb contour, pressures are locally higher than under the positive mode, when fewer systems are found.

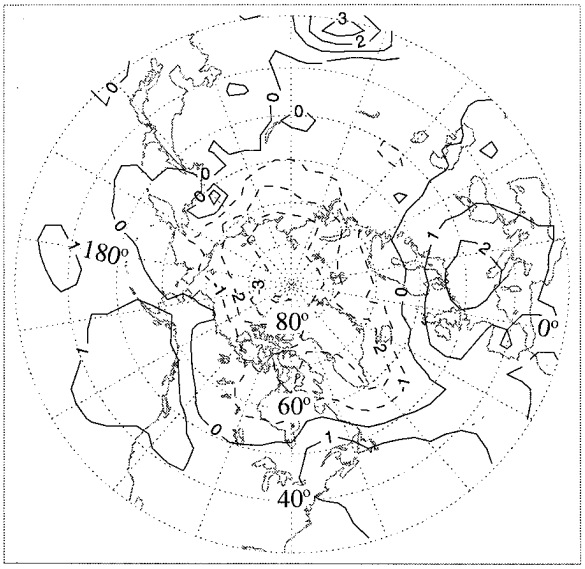

FIG. 7. Difference field of mean SLP for the cold season, 1983/84–1992/93 minus 1973/74–1982/83. Positive differences are shown by solid contours with negative differences shown by dashed contours.

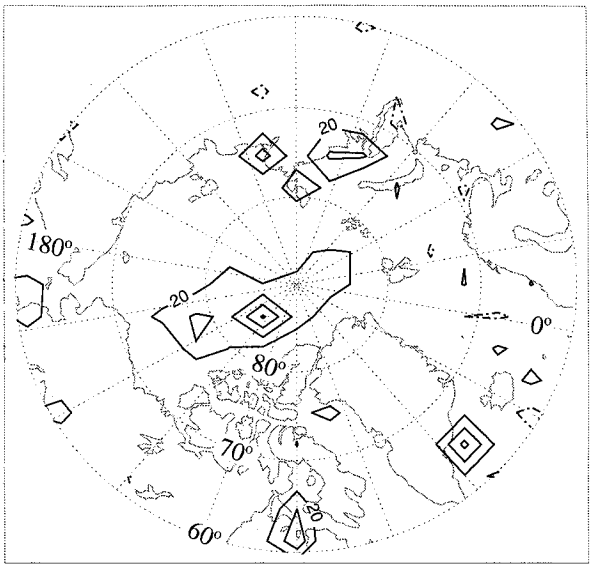

FIG. 8. Difference field of cyclone events north of 60°N for the cold season, 1983/84–1992/93 minus 1973/74–1982/83. The contour interval is 20. Positive differences are shown by solid contours with negative differences shown by dash–dot contours.

b. Recent changes

Since about 1970, the NAO index during winter has changed from a predominantly negative to a positive mode, with several particularly large positive values since about 1980 (Hurrell 1995b) but with large variability. Our analyses (not shown) reveal that this pattern holds for the longer cold season (October–March) as well. We would consequently expect decreases (increases) in SLP in the IL (AH) regions, with corresponding increases in IL cyclone activity. A difference map (Fig. 7) of cold season mean SLP north of 30°N between the most recent decade (1983/84 to 1992/93) and the previous decade (1973/74 to 1982/83) reveals that intensification of the IL and AH is only part of a larger-scale shift in circulation. Mean pressures in the climatological IL have decreased by about 2.5 mb, with corresponding increases of 1.5 mb in the vicinity of the AH. Increases are also observed over central Europe, the northeastern Pacific and south-central Asia over the Himalayas (the latter, covering a small area but with tight gradients is possibly spurious, related to reduction of pressure to sea level). However, decreased pressures dominate the Arctic, with the maximum exceeding 4 mb centered near the pole. Walsh et al. (1996) have examined these central Arctic pressure reductions more closely using data for the period 1979–94, and note that the SLP changes between 1987–94 and 1979–86 are largest and statistically significant for autumn and winter means. With respect to the 16-yr mean, annual pressures have been below normal in every year since 1988.

Figure 8 provides the corresponding difference map of latitude-weighted cold season cyclone counts for the region north of 60°N. A general correspondence is observed between the SLP decreases and increased high-latitude storm activity. For the region north of 60°N as a whole, a two-tailed *t* test of the change in cyclone counts between the two periods, using as before counts normalized to the 28-yr monthly means, reveals the increase as significant at the 0.01 level. Note in particular the correspondence between the increases in cyclone activity near the pole and the region of maximum SLP change. Additional two-tailed *t* tests, performed for counts over a 28-gridpoint region encompassing the 20 event contour near the pole reveals this increase to be locally significant (0.01). The changes near the Kara Sea (over a 24 gridpoint region) and the southern Canadian Arctic Archipelago (over a 9-gridpoint region) are also locally significant. However, those over the 12-point IL region are not significant, which reflects the high variability in the NAO. Significant increases in cyclone activity over the central Arctic Ocean are also found for the warm season.

Time series of cold-season cyclone counts for the region north of 60°N and for 30°–60°N (Fig. 9) show that the increase in northern high latitudes is most pronounced from the early 1980s onward. An analysis for the region north of 65°N (not shown), which largely eliminates IL cyclones, shows the same increasing tendency. The warm season as evaluated north of 60°N (not shown) reveals a more general increase since 1966. Cold season cyclone activity for lower latitudes decreased from 1966/67 to 1975/76, but with generally high values in the subsequent decade, with low values from 1988/89 onward. In an earlier analysis, Serreze et al. (1993) showed statistically significant increases in cyclone activity north of 65°N over the period 1952–

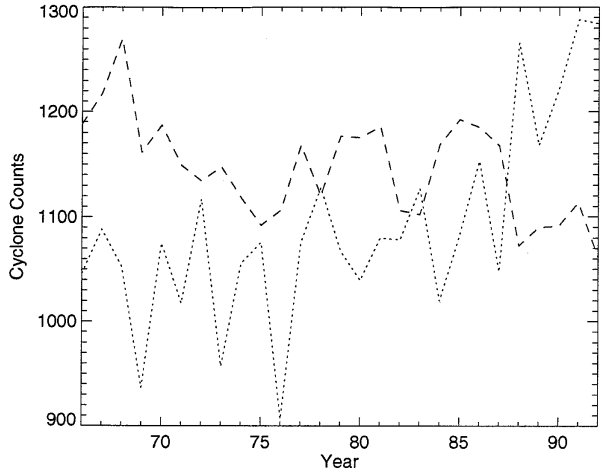

FIG. 9. Time series of cold season cyclone counts (1966/67 to 1992/93) for north of 60°N (dotted lines) and for 30°–60°N (dashed lines). To display both time series on the same scale, counts for the 30°–60°N zonal band have been divided by two.

89 for winter, spring, and summer. Our results suggest that this upward tendency in high latitudes has continued, which at least in recent years, is dominated by changes over the central Arctic Ocean as opposed to the IL. Trenberth (1990) notes a large shift in the winter circulation in the North Pacific characterized by a deeper and eastward displaced Aleutian low for the period 1977–87 compared with 1946–76, with reductions in SLP over the northern North Pacific of more than 4 mb. Our analysis of differences in SLP and cyclone activity for December–January of 1977–87 minus 1966–76 show this change, but this tendency has not been maintained subsequently.

In evaluating these changes, one must be aware of possible temporal inhomogeneities in the SLP record. In particular, Arctic analyses have improved since 1979, when data from the International Arctic Buoy Program began to be incorporated into NMC analyses (Colony and Rigor 1993). It will hence be instructive to repeat our calculations using the consistent 40-yr record soon to be available through the National Center for Environmental Prediction (formerly NMC)/National Center for Atmospheric Research (NCEP/NCAR) ''reanalysis'' project (Kalnay et al. 1996). However, other lines of evidence support our conclusions.

Chapman and Walsh (1993) note that increases in Northern Hemisphere surface temperatures since 1961 have been largest during winter and spring over the subpolar land areas of Alaska, northwestern Canada, and over northern Eurasia, whereas cooling is indicated over southern Greenland and the western subpolar North Atlantic. Hurrell (1995b) shows essentially the same pattern of temperature change for winters 1981–93. He argues that the cooling near Greenland and warming over Scandinavia, Northern Europe, the former Soviet Union, and much of central Asia are consistent with recent increases in the NAO index. Although this view seems supported with regard to the cooling near Greenland and warming over Scandinavia and northern Europe, Rogers and Mosley-Thompson (1995) argue that the recent mild winters over north-central Asia do not correspond with the NAO, but are instead related to stronger westerly flow and extensive cyclone warm sectors entering this region. The observed recent increases in cyclone activity over the Kara Sea, which should promote southerly advection into this region, supports this view. Note that system counts corresponding to the positive NAO mode (Fig. 6) tend to decrease over the Kara Sea. As the NAO has become more positive, the recent increase in Kara Sea activity would not be expected.

According to Trenberth (1990) and Trenberth and Hurrell (1994), observed increases in winter surface temperatures over Alaska from about 1977–88 can be related to the deeper and eastward-shifted Aleutian low during this period advecting warm, moist Pacific air along the west coast of North America and into Alaska. The pattern of pressure changes shown in Fig. 7 suggests a more recent shift toward westerlies, in turn associated with increased cyclone activity over the central Arctic Ocean. In also providing a generally maritime airmass source, this could help explain why temperatures have continued to be anomalously high in this region.

As noted, the recent increases in cyclone activity over the central Arctic also hold for the warm season. Serreze et al. (1995b) argue that the record minimum in sea ice area observed during 1990, exemplified by extensive open water north of Siberia during August, was in large part initiated by persistent cyclone activity over the central Arctic during May 1990, resulting in early melt, wind-driven breakup of the pack ice, and consequent reductions in surface albedo. In a subsequent study, Maslanik et al. (1996) show that the ice conditions in 1990 are part of a general pattern of summertime reductions north of Siberia in recent years, consistent with the more frequent invasions of warm air and poleward ice advection by offshore winds associated with the enhanced central Arctic cyclone pattern. Although the tendency for increased cyclonic vorticity to promote sea ice divergence suggests that these coastal ice losses are attended by reductions in sea ice concentration over the perennial pack ice (Walsh et al. 1996), this issue remains to be explored.

5. Summary and conclusions

Output from an automated cyclone detection and tracking algorithm, applied to twice-daily NMC fields for the period 1966–93, is used to examine the characteristics of cyclone activity associated with the IL, the North Atlantic Oscillation, and recent changes in the IL in relation to the larger Northern Hemisphere circulation. The major findings are summarized as follows.

1) Only a modest seasonal cycle is observed in the

frequency of cyclones in the IL region, with the highest counts during winter. Stronger seasonal cycles are observed in cyclone intensity and maximum deepening rates.

2) For the cold season, IL cyclones have intensities typical of oceanic systems over both the Atlantic and Pacific, but with a generally lower frequency of pronounced and extreme deepening rates. During the warm season, IL cyclone intensities are typical of Northern Hemisphere values, with deepening characteristics typical of most oceanic regions.

3) Depending on the month, from 10% to 15% of all cyclone events in the IL region represent within-region cyclogenesis. In general, a somewhat higher fraction is represented by local cyclolysis. For most months, over half of all systems associated with the IL show their first appearance of a closed isobar north of 55°N. However, for both the warm and cold seasons, IL cyclones can occasionally be tracked upstream as closed systems as far as the northern and southern Rocky Mountains, with a larger contribution from the U.S. Atlantic seaboard.

4) Composite analyses for the cold season show an increase (decrease) in system counts over the climatological IL region by more than a factor of 2 during positive (negative) extremes of the NAO. No change is observed in the percentage of cyclone events represented by within-region cyclogenesis, cyclolysis, or migration from lower latitudes. Cyclone intensifies are greater during the positive mode.

5) Increases in cyclone activity during the positive mode are primarily limited to the climatological IL region itself. During the negative mode, cyclone activity increases over the Atlantic from about 40° to 60°N. However, the increases in activity to the south are comparatively modest, broadly consistent with the southward shift and weakening of the subpolar low.

6) Despite the generally more positive NAO index in recent years for the cold season, cyclone activity in the climatological IL region has not significantly increased. However, there have been significant increases for the region north of 60°N as a whole, with locally significant increases over the central Arctic Ocean, the Kara Sea, and the Canadian Arctic Archipelago. These changes are accompanied by decreases in mean SLP, which are largest near the pole. Similar changes are observed over the central Arctic during the warm season. Generally opposing changes are found for 30°–60°N. These recent changes are consistent with observed patterns of surface temperature over northern high latitudes and reductions in Arctic sea ice area.

Acknowledgments. This study was supported by NSF Contracts ATM-9315351, OPP-9321547, OPP-9504201, NOAA Contracts NA36GP0236 and NA56GP0213, and undergraduate student internship support to F. Carse through a Colorado Commission on Higher Education grant to CIRES. The anonymous reviewers are thanked for their helpful comments.

REFERENCES

Angell, J. K., and J. Korshover, 1974: Quasi-biennial and long-term fluctuations in centers of action. *Mon. Wea. Rev.*, **102,** 669–678.

Barnston, A. G., and R. E. Livezey, 1987: Classification, seasonality, and persistence of low-frequency atmospheric circulation patterns. *Mon. Wea. Rev.,* **115,** 1083–1126.

Blackmon, M. L., Y. Lee, and J. Wallace, 1984a: Horizontal structure of 500 mb height fluctuations with long, intermediate, and short time scales. *J. Atmos. Sci.,* **41,** 961–979.

Carleton, A. M., 1988: Meridional transport of eddy sensible heat in winters marked by extremes of the North Atlantic oscillation, 1948/49–1979/80. *J. Climate,* **1,** 212–223.

Chapman, W. L., and J. E. Walsh, 1993: Recent variations of sea ice and air temperature in high latitudes. *Bull. Amer. Meteor. Soc.*, **74,** 33–47.

Colony, R. L., and I. G. Rigor, 1993: International Arctic Buoy Program Data Report for 1 January 1992–21 December 1992. Applied Physics Laboratory Tech. Memo. APL-UW TM 29-93, 215 pp. [Available from Applied Physics Laboratory, University of Washington, 1013 NE 40th Street, Seattle, WA 98105-6698.].

Deser, C., and M. L. Blackmon, 1993: Surface climate variations over the North Atlantic Ocean during winter: 1900–1989. *J. Climate,* **6,** 1743–1753.

Hurrell, J. W., 1995a: Transient eddy forcing of the rotational flow during northern winter. *J. Atmos. Sci.,* **52,** 2286–2301.

——, 1995b: Decadal trends in the North Atlantic oscillation: Regional temperatures and precipitation. *Science,* **269,** 676–679.

Kalnay, E., and Coauthors, 1996: The NCEP/NCAR 40–Year Reanalysis Project. *Bull. Amer. Meteor. Soc.,* **77,** 437–471.

Maslanik, J. A., M. C. Serreze, and R. G. Barry, 1996: Recent decreases in Arctic summer ice cover and linkages to atmospheric circulation anomalies. *Geophys. Res. Lett.,* **23,** 1677–1680.

Moses, T., G. N. Kiladis, H. F. Diaz, and R. G. Barry, 1986: Characteristics and frequency of reversals in mean sea level pressures in the North Atlantic sector and their relationship to long term temperature trends. *J. Climatol.,* **7,** 13–30.

Murray, R. J., and I. Simmonds, 1991: A numerical scheme for tracking cyclone centers from digital data. Part I: Development and operation of the scheme. *Aust. Meteor. Mag.,* **39,** 155–166.

Pettersen, S., 1950: Some aspects of the general circulation of the atmosphere. *Centennial Proc. Roy. Meteor. Soc. London,* 120–155.

Putnins, P., 1970: The climate of Greenland. *World Survey of Climatology.* Vol. 14, *Climates of the Polar Regions,* S. Orvig, Ed., Elsevier, 3–128.

Roebber, P. J., 1984: Statistical analysis and updated climatology of explosive cyclones. *Mon. Wea. Rev.,* **112,** 1577–1589.

——, 1989: On the statistical analysis of cyclone deepening rates. *Mon. Wea. Rev.,* **117,** 2293–2298.

Rogers, J. C., 1990: Patterns of low-frequency monthly sea level pressure variability (1899–1986) and associated wave cyclone frequencies. *J. Climate,* **3,** 1364–1379.

——, and H. van Loon, 1979: The seesaw in winter temperatures between Greenland and northern Europe. Part II: Some ocean and atmospheric effects in middle and high latitudes. *Mon. Wea. Rev.,* **107,** 509–519.

——, and E. Mosley-Thompson, 1995: Atlantic Arctic cyclones and the mild Siberian winters of the 1980s. *Geophys. Res. Lett.,* **22,** 799–802.

Sahsamanoglou, H. S., 1990: A contribution to the study of action centres in the North Atlantic. *Int. J. Climatol.,* **10,** 247–261.

Sanders, F., and J. R. Gyakum, 1980: Synoptic–dynamic climatology of the ''bomb.'' *Mon. Wea. Rev.,* **108,** 1589–1606.

Serreze, M. C., 1995: Climatological aspects of cyclone development and decay in the Arctic. *Atmos.–Ocean,* **33,** 1–23.

——, J. E. Box, R. G. Barry, and J. E. Walsh, 1993: Characteristics of Arctic synoptic activity, 1952–1989. *Meteor. Atmos. Phys.*, **51,** 147–164.

——, J. A. Maslanik, J. R. Key, R. F. Kokaly, and D. A. Robinson, 1995: Diagnosis of the record minimum in Arctic sea ice area during 1990 and associated snow cover extremes. *Geophys. Res. Lett.*, **22,** 2183–2186.

Sinclair, M. R., 1994: An objective cyclone climatology for the Southern Hemisphere. *Mon. Wea. Rev.*, **122,** 2239–2256.

Trenberth, K. E., 1990: Recent observed interdecadal climate changes in the Northern Hemisphere. *Bull. Amer. Meteor. Soc.*, **71,** 988–993.

——, and J. G. Olson, 1988: Evaluation of NMC global analyses: 1979–1987. NCAR Tech. Note NCAR/TN-299+STR, 82 pp.

——, and J. W. Hurrell, 1994: Decadal atmosphere–ocean variations in the Pacific. *Climate Dyn.*, **9,** 303–319.

U.K. Meteorological Office, 1964: *The Northern Seas.* Vol. 1, Part 1, *Weather in Home Fleet Waters*, Her Majesty's Stationery Office, 265 pp.

van Loon, H., and J. C. Rogers, 1978: The seesaw in winter temperatures between Greenland and Northern Europe. Part I: General description. *Mon. Wea. Rev.*, **106,** 296–310.

Walker, G. T., 1923: Correlation in seasonal variations of weather, VIII: A preliminary study of world weather. *Mem. Ind. Meteor. Dept. (Poona),* **24,** 275–332.

——, and E. W. Bliss, 1932: World weather. *V. Mem. Roy. Meteor. Soc.*, **103,** 29–64.

Wallace, J. M., 1983: The climatological mean stationary waves; Observational evidence. *Large-Scale Dynamical Processes in the Atmosphere*, B. Hoskins and R. Pearce, Eds., Academic Press, 27–53.

Walsh, J. E., and R. G. Crane, 1992: A comparison of GCM simulations of Arctic climate. *Geophys. Res. Lett.*, **19,** 29–32.

——, W. L. Chapman, and T. L. Shy, 1996: Recent decrease of sea level pressure in the central Arctic. *J. Climate,* **9,** 480–486.

Whittaker, L. M., and L. H. Horn, 1984: Northern Hemisphere extratropical cyclone activity for four mid-season months. *J. Climatol.*, **4,** 297–310.